Report

Current Biology

# The Minimal Energetic Requirement of Sustained Awareness after Brain Injury

## Highlights

- Quantitative FDG-PET allows fine diagnosis and prognosis in disorders of consciousness
- Level of consciousness after brain injury correlates with whole-brain energetic state
- Emergence of awareness occurs above a sharply defined brain energy metabolic boundary

## Authors

Johan Stender, Kristian Nygaard Mortensen, Aurore Thibaut, Sune Darkner, Steven Laureys, Albert Gjedde, Ron Kupers

## Correspondence

kupers@sund.ku.dk

## In Brief

Stender et al. show that positron emission tomography measurement of whole-brain glucose metabolic state allows accurate diagnosis and prediction of disorders of consciousness. Recovery from the unresponsive wakefulness condition occurs above a sharply defined brain metabolic limit, reflecting the minimal energetic requirements of consciousness.

Stender et al., 2016, Current Biology *26*, 1494–1499
June 6, 2016 
http://dx.doi.org/10.1016/j.cub.2016.04.024

CellPress

CellPress

Current Biology
Report

# The Minimal Energetic Requirement of Sustained Awareness after Brain Injury

Johan Stender,[1,2,5] Kristian Nygaard Mortensen,[1,5] Aurore Thibaut,[2] Sune Darkner,[3] Steven Laureys,[2] Albert Gjedde,[1] and Ron Kupers[1,4,*]

[1]BRAINlab, Department of Neuroscience & Pharmacology, Panum Institute, University of Copenhagen, Nørre Allé 10, 2200 Copenhagen, Denmark

[2]Cyclotron Research Center and Department of Neurology, CHU Sart Tilman, University of Liège, Avenue de l'hôpital 11, 4000 Liège, Belgium

[3]Department of Computer Science, University of Copenhagen, Universitetsparken 5, 2100 Copenhagen, Denmark

[4]Department of Radiology & Biomedical Imaging, Yale University, 300 Cedar Street, New Haven, CT 06520, USA

[5]Co-first author

*Correspondence: kupers@sund.ku.dk

http://dx.doi.org/10.1016/j.cub.2016.04.024

## SUMMARY

**Differentiation of the minimally conscious state (MCS) and the unresponsive wakefulness syndrome (UWS) is a persistent clinical challenge [1]. Based on positron emission tomography (PET) studies with [$^{18}$F]-fluorodeoxyglucose (FDG) during sleep and anesthesia, the global cerebral metabolic rate of glucose has been proposed as an indicator of consciousness [2, 3]. Likewise, FDG-PET may contribute to the clinical diagnosis of disorders of consciousness (DOCs) [4, 5]. However, current methods are non-quantitative and have important drawbacks deriving from visually guided assessment of relative changes in brain metabolism [4]. We here used FDG-PET to measure resting state brain glucose metabolism in 131 DOC patients to identify objective quantitative metabolic indicators and predictors of awareness. Quantitation of images was performed by normalizing to extracerebral tissue. We show that 42% of normal cortical activity represents the minimal energetic requirement for the presence of conscious awareness. Overall, the cerebral metabolic rate accounted for the current level, or imminent return, of awareness in 94% of the patient population, suggesting a global energetic threshold effect, associated with the reemergence of consciousness after brain injury. Our data further revealed that regional variations relative to the global resting metabolic level reflect preservation of specific cognitive or sensory modules, such as vision and language comprehension. These findings provide a simple and objective metabolic marker of consciousness, which can readily be implemented clinically. The direct correlation between brain metabolism and behavior further suggests that DOCs can fundamentally be understood as pathological neuroenergetic conditions and provide a unifying physiological basis for these syndromes.**

## RESULTS

Positron emission tomography (PET) studies with [$^{18}$F]-fluorodeoxyglucose (FDG) suggest that impaired consciousness following brain injury is associated with overall brain metabolic levels of 40%–60% of normal in conditions of coma, unresponsive wakefulness syndrome (UWS), and minimally conscious state (MCS) [5, 6]. Notwithstanding, relative regional variations in metabolism correlate with the preservation of specific behavioral or perceptual functions in MCS patients [7, 8], supporting the claim that network activations cause local increases in energy metabolism even in disorders of consciousness (DOCs) [9]. Although assessment of relative cerebral metabolic patterns with FDG-PET is a sensitive diagnostic tool in DOCs, current methods are non-quantitative and inherently examiner dependent. The development of diagnostic markers based on quantitative measures of brain metabolism would enable a more objective method for diagnosing DOCs, but they necessitate the establishment of absolute energetic requirements of awareness. However, no absolute cerebral metabolic criteria exist that allow to distinguish between MCS and the more severe UWS [1, 6], mainly because the presence of severe brain pathology interferes with conventional non-invasive quantification methods. We therefore employed a method of FDG uptake normalization relative to extracerebral tissue, developed specifically to accommodate difficulties in PET imaging of severe brain injury patients. We hypothesized that global glucose metabolic activity predicts the capacity for maintenance of conscious awareness, while its regional variations reflect the integrity of specific perceptual or cognitive functions. We also test the hypothesis that the global cerebral metabolic rate predicts the preservation or reattainment of consciousness at 1-year follow-up.

FDG-PET data at rest were acquired in 131 DOC patients and 28 healthy controls (Table 1). The patient population was split into independent cohorts for derivation and validation of the diagnostic model (Table S1). PET images were normalized to signal intensity in the extracerebral cephalic tissue, which is unaffected by brain injury and stable across subjects, thus yielding a pseudo-quantitative cerebral metabolic index. To perform the normalization, a reference distribution was calculated from the extracerebral tissue intensity distributions of the 28 control subjects. Each individual image of the study population was

**Table 1. Patient Demographics**

| Study Cohort | CRS-R Diagnosis | n | Mean Age (Range, Y) | Male | Time since Onset Mean (Range, D) | Traumatic Etiology |
|---|---|---|---|---|---|---|
| Derivation | UWS | 14 | 43 (22–73) | 11 | 635 (7–2,884) | 3 |
| | MCS | 21 | 38 (15–66) | 13 | 1,013 (13–3,336) | 11 |
| Validation | UWS | 35 | 48 (21–75) | 20 | 622 (5–6,708) | 10 |
| | MCS | 44 | 41 (15–72) | 28 | 1,299 (23–9,595) | 22 |
| | EMCS | 17 | 35 (16–62) | 15 | 1,101 (143–5,080) | 11 |
| | control | 28 | 44 (20–70) | 16 | – | |
| | total | 159 | 42 (15–75) | 103 | 978 | 57 |

subsequently normalized, by selecting a global scaling factor of the image intensity such that the Jensen-Shannon divergence between the reference distribution and the subject's extracerebral intensity distribution was minimized [10]. Metabolic activity after normalization was assigned an index value, with average extracerebral metabolism in the reference distribution set to one (see Supplemental Experimental Procedures). Brain images were then first segmented into entire cerebral cortex of left and right hemispheres and then further according to Brodmann areas (BA) (Supplemental Experimental Procedures). We extracted the mean cortical FDG uptake in each hemisphere and BA volumes of interest (VOIs). We used the mean cortical metabolism of the best preserved hemisphere (with highest mean cortical metabolism prior to lesion masking) to classify between UWS and MCS and predict outcome at 1-year follow-up, using receiver operating characteristic (ROC) analysis.

## Global Glucose Metabolism Rate as Diagnostic Marker

Mean cortical metabolic index was 7.59 ± 1.19 in healthy controls, 2.88 ± 0.74 (38% of normal) in UWS, 4.23 ± 1.03 (56% of normal) in MCS, and 4.76 ± 0.65 (63% of normal) in emergence from MCS (EMCS). See Figure 1 for individual patient examples. One-way ANOVA with Bonferroni correction for three comparisons showed that average metabolic rates were significantly higher in MCS than UWS ($p < 0.001$) and in healthy controls compared to EMCS ($p < 0.001$), but not in EMCS compared to MCS ($p = 0.098$). Metabolic rates were not influenced by any of a range of possible confounders, including age, etiology, time since onset, and use of sedation during imaging (Supplemental Experimental Procedures).

Average cortical glucose metabolism gave diagnostic discrimination between MCS and UWS at an area under the ROC-curve (AUC) of 0.84 (confidence interval [CI] 0.67–1) in the derivation cohort and 0.91 (CI 0.84–0.98) in the validation cohort. The performance of the classifier did not significantly differ between the two cohorts ($p = 0.45$). The best classification rate in the derivation cohort was achieved at a metabolic index of 3.17 (41% of normal activity; Figure 2), resulting in 89% correct classification between UWS and MCS, with 95% sensitivity and 79% specificity to MCS, thus satisfying reasonable requirements for a clinically useful diagnostic criterion. In the validation cohort, this diagnostic threshold provided an 87% correct classification rate between UWS and MCS, with 95% sensitivity and 77% specificity to MCS. Post hoc inference suggested an optimal metabolic cutoff at a metabolic index of 3.19 (42% of normal) in the validation cohort; all patient classifications at this level remained unchanged compared to the derivation cohort threshold, i.e., performance of the diagnostic model was similar in the derivation and validation cohorts (Table 2).

Diagnostic accuracy with the above diagnostic criterion provided an AUC of 0.89 across the pooled cohort (CI 0.82–0.96). There was 88% correct classification between MCS and UWS, with 95% sensitivity and 78% specificity to MCS. Every EMCS patient and healthy control was correctly identified as conscious.

## Outcome Prediction

Outcome data at 1-year follow-up were obtained for 91% of the patients. Demographic and clinical data did not differ between patients with known outcome data and those without follow-up data. Group discrimination by the metabolic criterion correctly predicted 88% of all known patient outcomes, with 95% sensitivity and 76% specificity to manifest consciousness at follow-up (Figure 2; Table S3). A total of 11 UWS patients had brain metabolism above the 41% diagnostic threshold. Of these, eight had recovered consciousness at follow-up, and the remaining three had died. One UWS patient with sub-threshold metabolism progressed to MCS on follow-up. Of the three MCS patients with sub-threshold metabolism, one died, while another one had no change of clinical condition. The third patient was lost to follow-up (Figure 2).

## Regional Metabolic Activity

No specific regional drivers of the patients' condition could be identified, as the metabolic group differences were present in all VOIs (Figure 3). Relative regional variability around the mean activity was low, with interregional coefficients of variance (SD/mean) of 6% in UWS, 13% in MCS, 14% in EMCS, and 15% in controls.

FDG uptake in peristriate visual cortex (BA 18) had the highest individual regional classification rate across the pooled cohort, with an AUC of 0.90. This value, however, did not differ significantly from the overall hemispheric classification rate (0.89; $p = 0.11$). BA 18 classification rate (86%), sensitivity to MCS (94%), and outcome prediction (80%) were slightly inferior to classification by the entire hemisphere.

In order to test the hypothesis that regional variations relative to the resting baseline metabolism can reflect preservation of specific cognitive and sensory functions, we first normalized all images to their global best-hemisphere mean (GM). Next, we calculated Pearson correlation coefficients between visual awareness, defined by the Coma Recovery Scale-Revised (CRS-R) as the capacity for visual tracking, and GM normalized

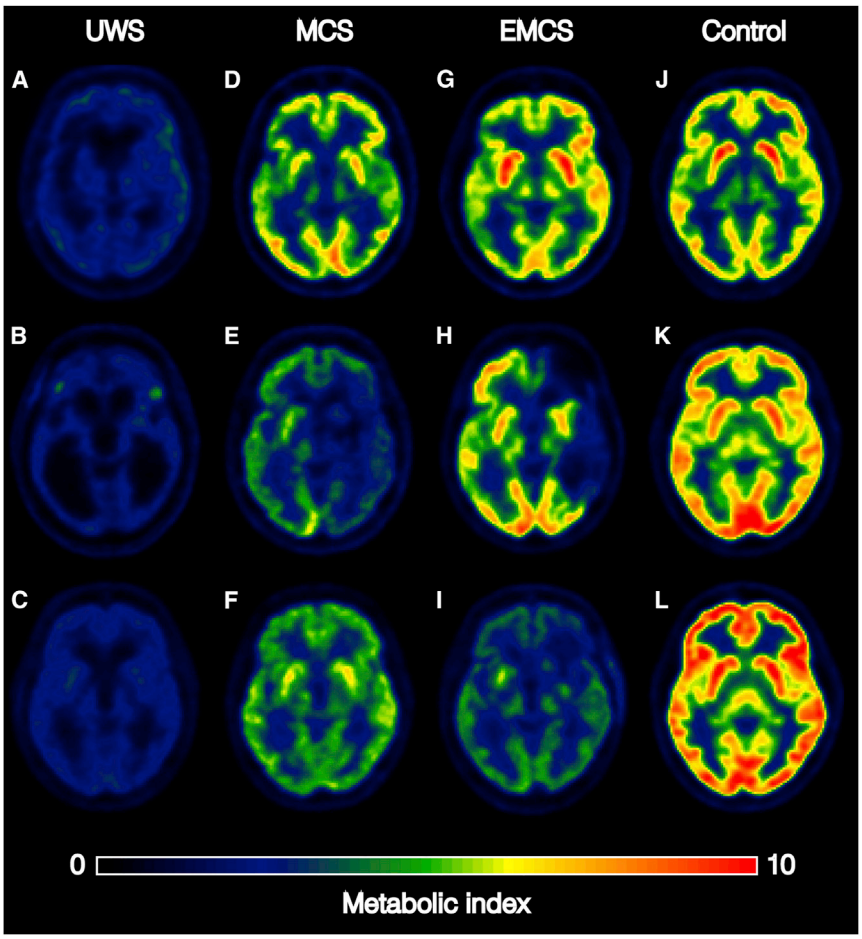


**Figure 1. Representative Individual FDG-PET Examples**

(A–C) UWS following subarachnoidal hemorrhage (A), traumatic brain injury (B), and anoxic brain injury (C), 8, 28, and 3 months after onset, respectively.

(D–F) MCS following traumatic brain injury (D), hemorrhagic stroke (E), and anoxic brain injury (F), 5 and 8 months and 3 weeks after onset, respectively.

(G–I) EMCS following traumatic brain injury with intracerebral hemorrhage (G), traumatic brain injury (H), and anoxic brain injury (I), 106, 68, and 2 months after onset, respectively.

(J–L) Healthy controls.

activity and absolute mean activity within visual cortex BAs 17, 18, and 19. Along the same line, we tested whether the ability to respond to verbal commands correlated with GM-normalized activity as well as absolute mean activity in areas commonly associated with receptive aphasia, i.e., the left primary and secondary auditory cortices (BAs 20–22) and Wernicke's area (BAs 39 and 40). Only MCS patients were included in this analysis. The presence of visual responsiveness correlated with GM-normalized metabolic rate in the visual cortex ($r = 0.24$, $p = 0.028$), but not with absolute metabolic rates ($r = 0.12$, $p = 0.29$). Capacity for command following correlated with both GM-normalized and extracerebral normalized metabolic index in the auditory and language-related areas ($r = 0.49$, $p < 0.0001$ and $r = 0.39$, $p = 0.002$, respectively).

## DISCUSSION

We tested the capacity of FDG-PET to diagnose the presence and to predict the recovery of consciousness in brain-injured subjects, using a novel measure of cerebral metabolic activity based on extracerebral tissue normalization. The model accuracy was determined in two independent cohorts, using both behavioral diagnosis and outcome at 1-year follow-up as references. We show that our index of cerebral metabolic activity differentiates accurately between UWS and MCS patients, hence providing a strong diagnostic and prognostic marker for chronic DOCs.

### Global Cortical Metabolism as Predictor of Consciousness

We hypothesized that the average cortical metabolic activity in the most intact cerebral hemisphere can be used to classify patients suffering from chronic DOCs. As large lateralized cerebral lesions are prevalent in this population and may selectively impair functioning of the affected hemisphere [11], global mean metabolic activity is a poor representation of preserved cerebral function. Since there is ample evidence that conscious awareness can be maintained with only one hemisphere [12, 13], we reasoned that an FDG-PET index of glucose metabolism of the least injured cortical hemisphere would be a better indicator of consciousness than is whole-brain cortical activity. This prediction was confirmed by our finding that mean glucose metabolism index in the best preserved hemisphere is an accurate subject-level diagnostic marker and that no individual brain region provided better classification than the average cortical signal. The diagnostic performance of this method was equally good in the derivation and validation samples, indicating that the method is valid across independent cohorts. ROC of the classification between MCS and UWS gave a common "optimal" diagnostic threshold of 42% of normal metabolic activity, resulting in excellent sensitivity and adequate specificity to MCS. Moreover, all EMCS patients and healthy controls were correctly identified as being conscious. We conclude that this FDG-PET diagnostic threshold provides reliable differentiation between conscious and unconscious subjects, with a good balance between type I and type II error risks.

The FDG metabolic index in the MCS groups largely overlapped with that in EMCS and was in a few cases within the range of healthy control values. This is not surprising given the fluctuating severity of MCS. Also, the mean cortical glucose metabolic index was not dependent on etiology or any of the potential confounders such as age or gender. Together, these results suggest that cerebral glucose metabolism is strongly linked to the expression of consciousness, irrespective of cause of injury

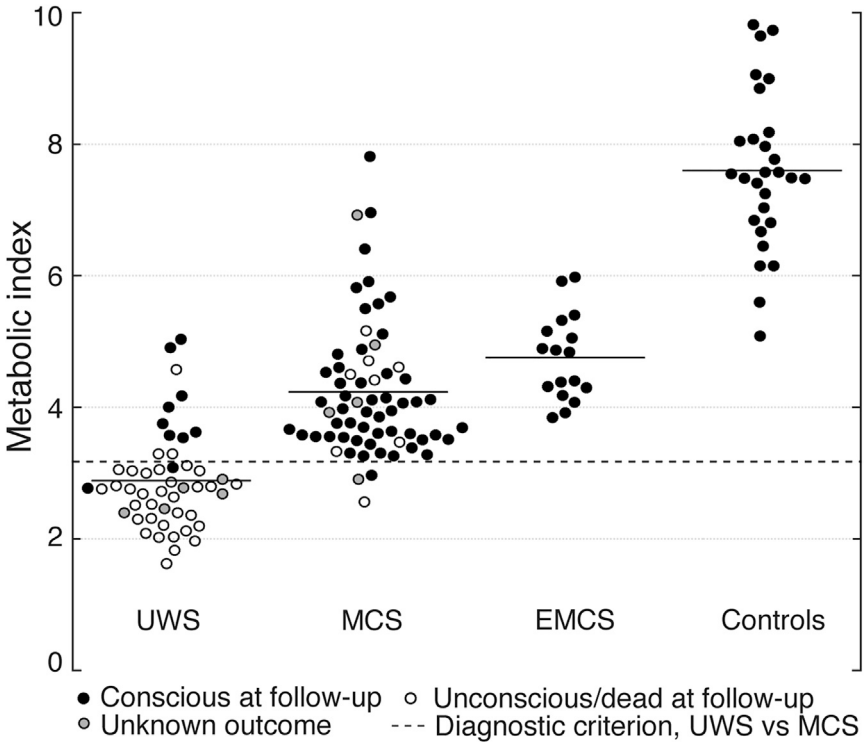


**Figure 2. Global Brain Glucose Metabolism**
Distribution of quantified cortical metabolic values (best preserved hemisphere) for all individual subjects in the pooled cohort. The dashed line marks the optimal diagnostic cutoff between patients in UWS and MCS. Horizontal lines mark the group averages. Metabolic values are indicated as a unitless index, with average activity in the scaling reference area (extracerebral tissue) set to 1. See also Tables S1–S3.

and time since onset. Cerebral metabolic activity also accurately predicted the level of consciousness at 1-year follow-up. Group separation along the 42% diagnostic threshold had an overall 88% correct outcome prediction in the mixed group of MCS and UWS patients. This is all the more compelling considering that the relatively high mortality rate over the long follow-up period may have attenuated the predictive power. Nonetheless, our method correctly predicted eight out of ten recoveries among UWS patients.

The specificity of the metabolic level to both diagnosis and prognosis suggests that the classification threshold represents the minimal energetic requirements of sustained awareness. Notably, our results indicate that transition between the unconscious and conscious states takes place above a sharply defined global (or hemispheric) metabolic boundary and point to a global energetic threshold effect, which enables the reemergence of consciousness after brain injury. This finding is consistent with previous propositions [2, 14] that consciousness cannot solely be attributed to activity in specific networks or areas but is associated with a whole-brain high energetic state. As such, preserved glucose metabolic rate in at least one hemisphere appears a necessary (but not sufficient) condition to regain awareness after brain injury. Overall, the cortical metabolic level accounted for the actual state or imminent recovery in 94% of the UWS and MCS patients. This direct correlation between brain metabolism and behavior indicates that global reduction of cortical neuronal work is a defining characteristic of DOCs and may provide a unifying physiological basis for these syndromes.

**Table 2. Diagnostic Discrimination between UWS and MCS by Cohort**

| Cohort | AUC | Highest Classification Rate | Optimal Metabolic Cutoff (Unitless Index) |
|---|---|---|---|
| Derivation | 0.84 (CI 0.67–1) | 0.89 | 3.17 |
| Validation | 0.91 (0.84–0.98) | 0.88 | 3.19 |
| Pooled | 0.89 (CI 0.82–0.96) | 0.88 | 3.18 |

## Significance of Regional Metabolic Variations Relative to the Cortical Hemispheric Average

All subjects had regional cerebral metabolic variations relative to the global mean signal. Brain activation in response to specific sensory or cognitive tasks can cause 10%–30% local increases in the magnitude of cortical glucose metabolism relative to resting baseline [9]. We reasoned that regions of relatively spared glucose metabolism in our patient groups reflect sustained activity in support of specific cognitive or sensory functions. Thus, while all conscious groups showed interregional variations with a coefficient of variance of 13%–15%, i.e., within the range of the proposed modular activation effect, glucose metabolic activity was nearly uniform across all cortical regions in UWS patients. Regional metabolic patterns in the MCS and EMCS groups were qualitatively similar to that observed in normal subjects, i.e., relatively higher in primary sensorimotor areas, although the peaks had lower absolute values and less variability. This pattern differs substantially from that of UWS patients, which was characterized by overall low FDG uptake, and is accordingly associated with capacity for consciousness. Our previous findings of relatively lowered frontoparietal metabolism in UWS patients [4, 6] can therefore be explained by the absence of regional activations rather than by a specific decline or injury to these areas.

MCS patients with absence of overt visual awareness had relatively lower activity in visual cortex, further supporting the functional relevance of regional variations in residual metabolism. Conversely, these patients' ability of command responding correlated with FDG uptake in auditory and language areas. Notably, these correlations emerged or became stronger after global mean scaling and therefore indicate relative preservation of energy metabolism in regions subserving preserved cognitive domains. Thus, with the global effect accounted for, specific regional differences between unconscious and conscious patients largely appear to reflect preserved sensory or cognitive capacity.

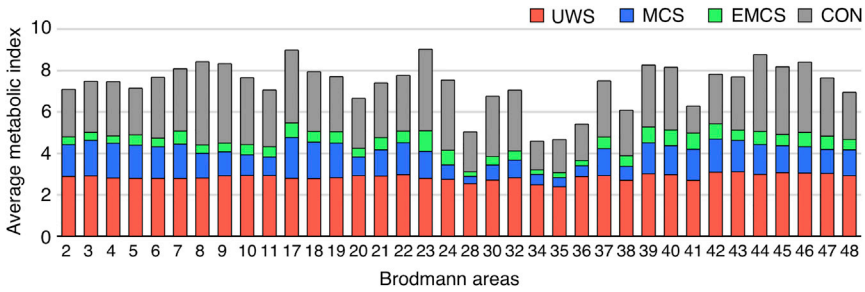


**Figure 3. Regional Variations in Brain Glucose Metabolism**

Average quantitative metabolic values by Brodmann area, for each diagnostic group, are represented on overlapping bars. Very small regions (<100 voxels) were excluded from the analysis.

## Clinical Implementation

The results indicate that assessment of cortical glucose metabolism by non-invasive FDG-PET is a reliable method for detecting the presence of, or potential for, consciousness and cognition after brain injury. The method is objective and computationally simple and provides easily interpretable results. Overall, this represents an important improvement to current non-quantitative diagnostic approaches with FDG-PET.

## Study Limitations

We here assume a direct correlation between the metabolic index and actual neuronal work. The accuracy of this assumption should be evaluated in further studies (but see Supplemental Experimental Procedures for supporting data). The present study was cross-sectional and did not allow evaluation of rapid evolution of metabolic status or their potential effects on clinical outcome. While we cannot attribute causation in the link between high brain glucose metabolism and conscious awareness, the FDG-PET literature on anesthesia [2, 3] suggests causation. We could not assess possible contributions of cerebral morbidity prior to injury, nor did we consider the normal declines in cerebral metabolism between childhood and adolescence [15] and further into old age [16].

The method requires high standards in image quality and registration. Current atlas-based approaches cannot precisely describe subcortical changes in severely deformed brains [17]. Investigations of subcortical metabolic drivers, such as thalamo-cortical [18] or mesocircuit loops [19], therefore fall outside the scope of this study.

## Conclusions

Hemispheric preservation of brain glucose metabolism predicts the presence, or potential for recovery, of consciousness in brain injury patients. Loci of regionally preserved metabolism subserve specific cognitive and sensory functions. The threshold of 42% of normal cortical hemispheric metabolic activity represents the minimal energetic requirement predictive of regaining consciousness. FDG-PET thus constitutes a strong diagnostic and prognostic marker in DOC arising from brain injury, irrespective of its pathogenesis.

## EXPERIMENTAL PROCEDURES

The study was approved by the Ethics Committee of the University Hospital of Liège, and all healthy controls and legal guardians of all participating patients gave written informed consent. Experimental procedures are described above. See Supplemental Experimental Procedures for details and methodological discussion. See also Figures S1–S4.

## SUPPLEMENTAL INFORMATION

Supplemental Information includes Supplemental Experimental Procedures, four figures, and three tables and can be found with this article online at http://dx.doi.org/10.1016/j.cub.2016.04.024.

## AUTHOR CONTRIBUTIONS

J.S., K.N.M., S.L., A.G., and R.K. conceived the study. J.S., A.T., and S.L. collected data. J.S., K.N.M., S.D., A.G., and R.K. analyzed data. J.S., K.N.M., and R.K. wrote the manuscript.

## ACKNOWLEDGMENTS

We note professional editing of the manuscript by Inglewood Biomedical Editing. The study was supported financially by the University of Copenhagen, the Belgian Fund for Scientific Research, the James S. McDonnell Foundation, the Belgian American Educational Foundation, the Wallonie-Bruxelles International, the European Commission, the European Space Agency, the Wallonia-Brussels Federation Concerted Research Action, and the Belgian interuniversity attraction pole.

Received: February 24, 2016
Revised: March 20, 2016
Accepted: April 8, 2016
Published: May 26, 2016

## REFERENCES

1. Laureys, S., and Schiff, N.D. (2012). Coma and consciousness: paradigms (re)framed by neuroimaging. Neuroimage *61*, 478–491.
2. Shulman, R.G., Hyder, F., and Rothman, D.L. (2009). Baseline brain energy supports the state of consciousness. Proc. Natl. Acad. Sci. USA *106*, 11096–11101.
3. Alkire, M.T. (1998). Quantitative EEG correlations with brain glucose metabolic rate during anesthesia in volunteers. Anesthesiology *89*, 323–333.
4. Stender, J., Gosseries, O., Bruno, M.-A., Charland-Verville, V., Vanhaudenhuyse, A., Demertzi, A., Chatelle, C., Thonnard, M., Thibaut, A., Heine, L., et al. (2014). Diagnostic precision of PET imaging and functional MRI in disorders of consciousness: a clinical validation study. Lancet *384*, 514–522.
5. Laureys, S., Owen, A.M., and Schiff, N.D. (2004). Brain function in coma, vegetative state, and related disorders. Lancet Neurol. *3*, 537–546.
6. Stender, J., Kupers, R., Rodell, A., Thibaut, A., Chatelle, C., Bruno, M.-A., Gejl, M., Bernard, C., Hustinx, R., Laureys, S., and Gjedde, A. (2015). Quantitative rates of brain glucose metabolism distinguish minimally conscious from vegetative state patients. J. Cereb. Blood Flow Metab. *35*, 58–65.
7. Bruno, M.-A., Majerus, S., Boly, M., Vanhaudenhuyse, A., Schnakers, C., Gosseries, O., Boveroux, P., Kirsch, M., Demertzi, A., Bernard, C., et al. (2012). Functional neuroanatomy underlying the clinical subcategorization of minimally conscious state patients. J. Neurol. *259*, 1087–1098.

8. Bruno, M.-A., Vanhaudenhuyse, A., Schnakers, C., Boly, M., Gosseries, O., Demertzi, A., Majerus, S., Moonen, G., Hustinx, R., and Laureys, S. (2010). Visual fixation in the vegetative state: an observational case series PET study. BMC Neurol. *10*, 35.

9. Shulman, R.G., Rothman, D.L., and Hyder, F. (1999). Stimulated changes in localized cerebral energy consumption under anesthesia. Proc. Natl. Acad. Sci. USA *96*, 3245–3250.

10. Lin, J.H. (1991). Divergence measures based on the Shannon entropy. IEEE Trans. Inf. Theory *37*, 145–151.

11. Bruno, M.A., Fernández-Espejo, D., Lehembre, R., Tshibanda, L., Vanhaudenhuyse, A., Gosseries, O., Lommers, E., Napolitani, M., Noirhomme, Q., Boly, M., et al. (2011). Multimodal neuroimaging in patients with disorders of consciousness showing "functional hemispherectomy". Prog. Brain Res. *193*, 323–333.

12. Carson, B.S., Javedan, S.P., Freeman, J.M., Vining, E.P., Zuckerberg, A.L., Lauer, J.A., and Guarnieri, M. (1996). Hemispherectomy: a hemidecortication approach and review of 52 cases. J. Neurosurg. *84*, 903–911.

13. Gazzaniga, M.S. (2005). Forty-five years of split-brain research and still going strong. Nat. Rev. Neurosci. *6*, 653–659.

14. Gjedde, A., Bauer, W.R., and Wong, D. (2011). Neurokinetics. In The Dynamics of Neurobiology In Vivo, A. Gjedde, W.R. Bauer, and D. Wong, eds. (Springer Verlag), pp. 241–290.

15. Kuzawa, C.W., Chugani, H.T., Grossman, L.I., Lipovich, L., Muzik, O., Hof, P.R., Wildman, D.E., Sherwood, C.C., Leonard, W.R., and Lange, N. (2014). Metabolic costs and evolutionary implications of human brain development. Proc. Natl. Acad. Sci. USA *111*, 13010–13015.

16. Cunnane, S., Nugent, S., Roy, M., Courchesne-Loyer, A., Croteau, E., Tremblay, S., Castellano, A., Pifferi, F., Bocti, C., Paquet, N., et al. (2011). Brain fuel metabolism, aging, and Alzheimer's disease. Nutrition *27*, 3–20.

17. Fridman, E.A., Beattie, B.J., Broft, A., Laureys, S., and Schiff, N.D. (2014). Regional cerebral metabolic patterns demonstrate the role of anterior forebrain mesocircuit dysfunction in the severely injured brain. Proc. Natl. Acad. Sci. USA *111*, 6473–6478.

18. White, N.S., and Alkire, M.T. (2003). Impaired thalamocortical connectivity in humans during general-anesthetic-induced unconsciousness. Neuroimage *19*, 402–411.

19. Schiff, N.D. (2010). Recovery of consciousness after brain injury: a mesocircuit hypothesis. Trends Neurosci. *33*, 1–9.

**Current Biology, Volume *26***

## Supplemental Information

# The Minimal Energetic Requirement of Sustained Awareness after Brain Injury

**Johan Stender, Kristian Nygaard Mortensen, Aurore Thibaut, Sune Darkner, Steven Laureys, Albert Gjedde, and Ron Kupers**

**Supplemental figures**

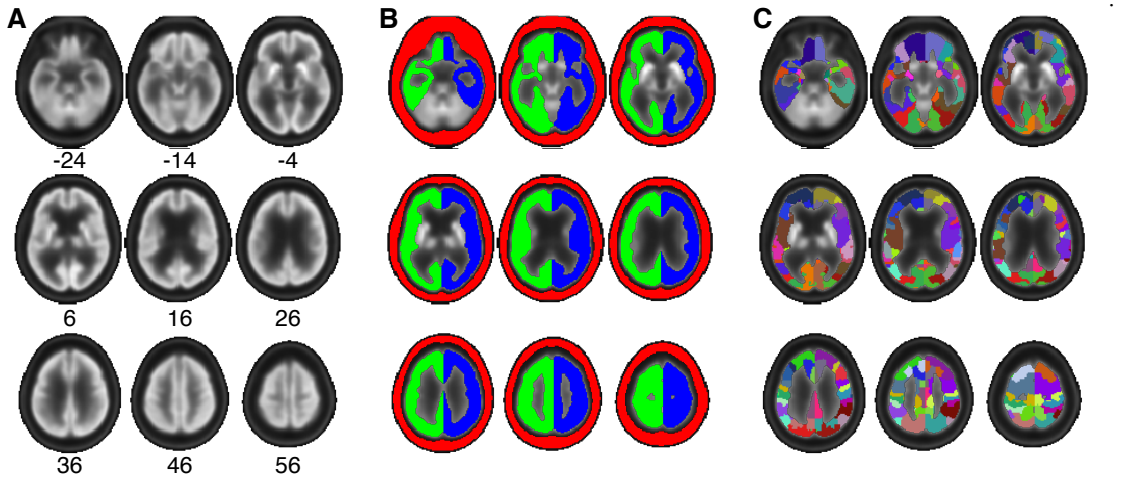


**Figure S1:** Template and segmentation masks. Related to Methods. (A) Template image. (B) Cortical hemisphere masks. (C) Brodmann area masks.

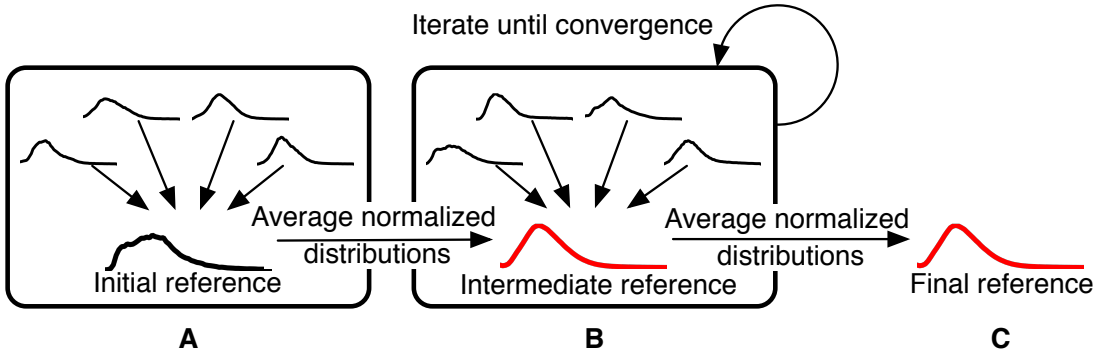


**Figure S2:** Reference distribution creation workflow. Related to Methods. (A) All distributions are fitted to a single-subject reference distribution, and averaged to the intermediate reference distribution. (B) Fitting to intermediate reference distribution and averaging is repeated until convergence, producing the final reference distribution (C).

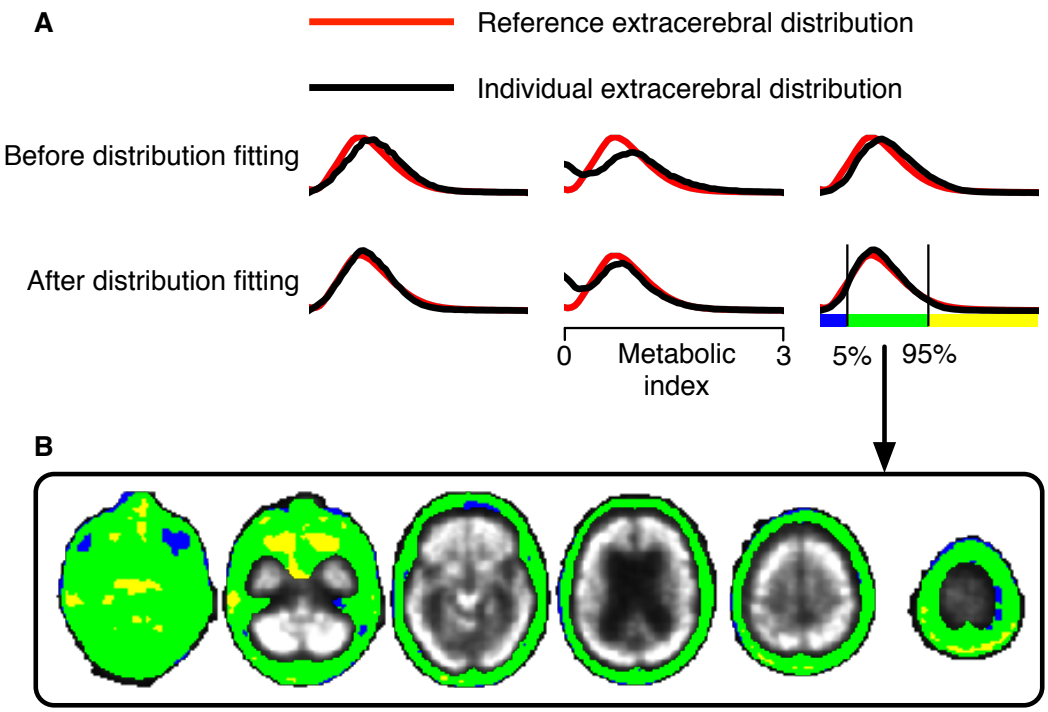


**Figure S3:** (A) Examples of extracerebral distributions after mean normalization (top) and distribution fitting (bottom). Related to Methods. (B) Spatial distribution of the 5$^{th}$ lowest (blue) and highest (yellow) percentile of voxels within the extracerebral mask for a single subject.

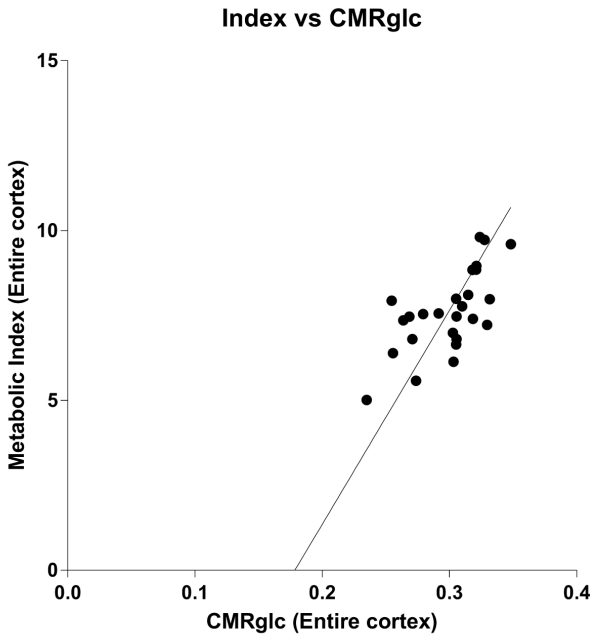


| | |
|---|---|
| Best-fit values ± SE | |
| Slope | 62.98 ± 14.11 |
| Y-intercept | -11.24 ± 4.243 |
| X-intercept | 0.1786 |
| 1/slope | 0.01588 |
| | |
| 95% Confidence Intervals | |
| Slope | 33.86 to 92.1 |
| Y-intercept | -20 to -2.488 |
| | |
| Is slope significantly non-zero? | |
| F | 19.92 |
| DFn, DFd | 1, 24 |
| P value | 0.0002 |
| Deviation from zero? | Significant |
| | |
| Equation | Y = 62.98*X - 11.24 |

**Figure S4:** Deming regression of average cortical metabolic values in 26 healthy controls, obtained with extracerebral normalization, and Sokoloff-modeling with a standard input-function. Related to Methods.

**Supplemental tables**

**Table S1:** Physiological covariants of metabolism. Related to Figure 2.

| **Measure** | **Cohort** | **p-value** |
|---|---|---|
| Age | Pooled | 0.984 |
| Etiology | Pooled | 0.123 |
| Time since onset | Pooled | 0.056 |
| Age | Derivation | 0.634 |
| Traumatic | Derivation | 0.786 |
| Time since onset | Derivation | 0.257 |
| Blood sugar | Derivation | 0.626 |
| Weight | Derivation | 0.545 |
| Dose | Derivation | 0.810 |
| Delay | Derivation | 0.601 |

**Table S2:** Effects of lesion masking. Related to Figure 2.

| **Diagnosis** | **Average highest hemispheric metabolic index before lesion masking** | **Average highest hemispheric metabolic index after lesion masking** | **Difference between results before and after masking (p-value)** |
|---|---|---|---|
| UWS | 2.880 | 2.882 | 0.987 |
| MCS | 4.220 | 4.234 | 0.944 |
| EMCS | 4.756 | 4.756 | 0.999 |

**Table S3:** 1-year outcomes of UWS and MCS patients. Related to Figure 2.

| | | CRS-R results | |
|---|---|---|---|
| | | UWS | MCS |
| PET-result | UWS | 2 conscious<br>31 unconscious (18 dead)<br>5 unknown | 1 conscious<br>1 unconscious (1 dead)<br>1 unknown |
| | MCS | 8 conscious<br>3 unconscious (3 dead) | 51 conscious<br>7 unconscious (7 dead)<br>4 unknown |

## SUPPLEMENTAL EXPERIMENTAL PROCEDURES

### Data transparency

Many of the patients were included in previous studies cited by this report. The derivation cohort of the present study was obtained from subjects included in [S1]. The validation cohort comprised patients included in [S1, S2] who underwent FDG-PET after 2010, as well as a number of more recently examined subjects. In total, 35 patients were included in [S1] and 75 in [S2].

### Supplemental methods

*Behavioral diagnosis*

The Coma Recovery Scale- Revised (CRS-R) is a sensitive diagnostic tool that is routinely used to discriminate among patients with very low levels of awareness [S3, S4]. Experienced neuropsychologists conducted daily CRS-R assessments over five consecutive days. The final diagnosis was determined by the best response obtained in the five assessments.

*Outcome assessment*

Twelve months following the initial CRS-R evaluation, long-term clinical outcome was assessed using the Glasgow Outcome Scale – Extended (GOS-E) [S5]. As we sought to predict the recovery of consciousness, the outcomes were ultimately stratified into the categories unconscious (GOS-E $\leq$ 2) or conscious (GOS-E > 2). Outcome evaluation was obtained from the patients' medical reports. The referring physician provided additional data when necessary.

*PET acquisition*

We acquired the PET data with a Gemini PET-CT (Philips Medical Systems) at the Liège University Hospital. Patients and controls were in a darkened and quiet room while receiving a bolus intravenous injection of FDG (185 - 370 MBq). After a 30-minute uptake phase, we recorded a single 12-minute emission frame. The images were corrected for attenuation using X-ray computed tomography (CT), as well as for random scatter and physical decay.

*PET registration and template creation*

PET images were registered to a population-specific PET template created separately for the patient (UWS and MCS combined) and control groups as described previously [S6]. In brief, all PET-FDG scans were first registered to the $H_2O$-PET-template provided in the SPM-software package [S6, S7], using an affine transformation, and then averaged to create an initial template. All individual PET-FDG images were registered to this template using affine and non-linear registration steps and then averaged, creating the next intermediate template. Registration to the previous intermediate template, and averaging, were repeated four times, resulting in the two final PET templates.

*Segmentation and parcellation*

We segmented the PET templates to left and right entire cerebral cortices, and extracerebral tissue, the latter being defined as tissue outside of the default SPM brain mask, with radioactivity concentration > 50% of the image wide mean activity. The bilateral cortical masks were then divided into volumes of interest (VOIs) for each Brodmann area (BA) using the brain atlas in MRIcron [S8]. (Figure S1). Individual PET-images were registered to the appropriate template (for patients or healthy controls) with affine and non-linear registration steps; hemisphere and VOI masks were subsequently transformed to individual PET-space using the inverse transformation. Nine VOIs contained less than 100 voxels after transformation and were omitted from further analysis.

*Extracerebral tissue normalization*

The gold standard for quantification of cerebral metabolic rate for glucose entails fitting a dynamic FDG-PET recording relative to the measured arterial input function; this requirement can hardly be met in routine studies, and invasive arterial catheterization is rarely employed in unresponsive patients. Commonly, FDG uptake is normalized to that in some reference brain region, assumed to be unaffected by treatment or medical condition [S9]. However, this assumption is clearly violated in brain-injured patients who present with global metabolic deficits and/or extensive lesions. An alternative approach, previously employed in [S1], substitutes

the individual arterial tracer curve with a standardized uptake curve obtained from a group of healthy volunteers. This approach assumes comparable uptake curves among subjects, a condition which may not be met, particularly in a population with heterogeneous brain-injuries. Also, substitution of a key physiological variable will invariably bias individual modeling results to some degree. Given these considerations, we developed a method for normalization of brain uptake to an extracerebral tissue, rather than to a brain reference region.

To perform the extracerebral normalization, a reference distribution was calculated from the 28 control subjects. All extracerebral intensity distributions of the control images were normalized to a randomly selected subject's extracerebral intensity distribution, by selecting a global scaling factor of the intensities such that the Jensen–Shannon divergence (JSD) between the distributions was minimized. A new distribution was then created as the average of the normalized distributions (Figure S1A). The process was iterated with the new average distribution as reference (Figure S1B-C) until a JSD between two subsequent reference distributions of less than $10^{-6}$ was obtained. Each individual image of the study population was subsequently normalized, by scaling the image intensities to minimize the JSD between the reference distribution and the subject's extracerebral distribution. The discrete distributions were approximated using 500 bin histograms, and the JSD minimized using the Nelder-Mead simplex minimization-method [S10]. Metabolic activity after normalization was assigned an index value, with average extracerebral metabolism in the reference distribution set to one (Figure S2). This approach assumes comparable individual glucose uptake in the extracerebral cranial volume, largely comprising bone, skin, blood, muscles and mucosa. Metabolic activity in these tissues is unaffected by brain pathology, rather uniform and of low inter-individual variability, and seemingly insensitive to physiological confounders [S11]. While this extracerebral signal might increase focally with muscle activity or inflammation, our procedure minimized the divergence between extracerebral intensities. The presence of divergent regions would elongate the tail of the voxelwise-distribution of FDG-uptake, but not otherwise affect distribution shape. As such, we contend that the extracerebral tissue signal is a valid normalization reference, and is in principle analogous to other methods for non-invasive quantitation [S12, S13]. Indeed, we found that hemispheric glucose metabolism was reduced to 37% in UWS, 56% in MCS, and 63% in EMCS groups, findings which match with previous results using more invasive quantitation [S1, S14, S15]. The low variability of cerebral FDG uptake among our healthy controls is also in line with previous findings [S16, S17]. Taken together, our extracerebral normalization results thus have face validity and are robust to the lack of a suitable cerebral reference region in these patients.

*Control for normalization and physiological confounders*

The normalization procedure assumes comparable shapes of the extracerebral intensity distribution across subjects. The normalization is primarily driven by the peak of the distribution curve, and thus requires a unimodal intensity distribution within the reference mask. Individual curve inspection indicated that the distribution peak was primarily driven by the vascular signal. Contributions from muscle and unvascularized volumes, in particular skull and cerebrospinal fluid, comprised a minor fraction of the full distribution volume. Differences in head-shape, or anatomical volume included in the image window did not affect curve shapes significantly (Figure S3).

To control for physiological confounders, contributions of age, weight, blood glucose levels, tracer dose and circulation time were tested in separate general linear models, with mean hemisphere uptake as dependent variable, and subject diagnosis as covariant. We further tested the stability of the normalization procedure to a priori parameters; histogram bin count and choice of initial subject for RD creation. To this end, we measured the average coefficient of variation (CV; std/mean) of global cerebral mean metabolism after normalization for all patients across different bin counts (100, 300, 600, 900), and different initial subject (all control subjects).

None of the tested physiological confounders correlated significantly with metabolism (Table S1). Differences in bin size provided negligible differences in final result of ED normalization (average CV: 2.2%). Similarly, the choice of the first subject in the creation of the RD had minor influence on the results (average CV: 3% across all possible initial subjects).

*Correspondence between the metabolic index and actual rate of glucose consumption*

To test the correspondence of the derived metabolic index to actual glucose metabolism, we further performed a Deming-correlation [S18] between average cortical metabolic values obtained in healthy volunteers, using Sokoloff-modeling with a standard arterial input function, and extracerebral normalization (Figure S4). Quantitation with a standard arterial input-function is generally accepted as a valid approximation of true kinetic modeling, although with some error at the individual level. Despite expected noise in both datasets, this analysis showed high correspondence ($r=0.68$, $p=0.0002$) between the extracerebral normalization results

and the approximated absolute metabolic rates of glucose. Overall, the above indicates that our findings are not specific to the normalization method, but could in principle be derived with any FDG-PET quantitation method, as long as the challenges of imaging in the severely injured brain are properly addressed.

*Effects of lesion masking*

For each patient group, we assessed the influence of focal lesions on the mean cortical FDG index by comparing its average metabolism with and without lesion masking, using the Wilcoxon rank-sum test. We controlled for confounds from age, gender, etiology, and time since onset, using separate general linear models with mean metabolism in the better hemisphere as dependent variable, and subject diagnosis as covariant. Lesion masks were required in 25 subjects, comprising on average 2% (range 0.5-15%) of the total volume in the best cortical hemisphere mask. Inclusion of the lesion masks did not significantly alter group mean cortical metabolism results or classifier performance (Table S2).

*Influence of anesthesia during the imaging protocol*

All patients were in a medically stable condition; none were intubated or in pharmacological coma during the behavioral examinations or at the start of the image acquisition. To avoid motion artifacts, a number of patients required sedation during the tomography. Sedation was in all cases performed with propofol, and initiated *after* tracer circulation. As the PET image predominantly reflects metabolic activity during the tracer circulation period, sedation during the tomography has negligible effects on the calculated FDG-uptake.

Corroborating this notion, we assessed the correlation between sedation during tomography and the calculated metabolic index with a linear regression, using diagnostic group as covariant. We here found no significant interaction between sedation and the metabolic index across the entire cohort ($p=0.186$). In total, only 9/49 (18%) UWS patients were sedated, compared to 27/65 (42%) and 8/17 (47%) of MCS and EMCS patients, respectively.

Within the UWS subgroup, the average metabolic index was significantly higher among sedated (3.49 ±0.99) than unsedated (2.75 ±0.61) subjects ($p=0.003$). We found no significant differences in average metabolic index between sedated (4.20 ±0.98) and unsedated (4.26 ±1.10) MCS patients ($p=0.83$). Likewise, we found no significant differences in average metabolic index between sedated (4.69 ±0.51) and unsedated (4.83 ±0.82) EMCS patients ($p=0.65$). We thus conclude that sedation during the imaging session is not a driving factor of the current results.

*Software packages*

Image registration and template creation were performed with Advanced Normalization Tools (ANTs version 2.0.3). Image processing and statistical analysis were performed in Matlab (Matlab 8.4 Mathworks Inc., Natick, Massachusetts) and STATA 12 (StataCorp. 2011. *Stata Statistical Software: Release 12*. College Station, TX: StataCorp LP), respectively. Data was used from the SPM8 Matlab toolbox (Statistical Parametric Mapping version 8, Wellcome Trust Centre for Neuroimaging, University of London) and the MRIcron software package (MRIcron version 6 june 2013, McCausland Center, University of South Carolina).

**Supplemental references**


[S1] Stender, J., Kupers, R., Rodell, A., Thibaut, A., Chatelle, C., Bruno, M.-A., Gejl, M., Bernard, C., Hustinx, R., Laureys, S., et al. (2015). Quantitative rates of brain glucose metabolism distinguish minimally conscious from vegetative state patients. J. Cereb. Blood Flow Metab. 35, 58-65.

[S2] Stender, J., Gosseries, O., Bruno, M.-A., Charland-Verville, V., Vanhaudenhuyse, A., Demertzi, A., Chatelle, C., Thonnard, M., Thibaut, A., Heine, L., et al. (2014). Diagnostic precision of PET imaging and functional MRI in disorders of consciousness: a clinical validation study. Lancet *9;384*, 514–522.

[S3] Hirschberg, R., and Giacino, J. T. (2011). The vegetative and minimally conscious states: diagnosis, prognosis and treatment. Neurol. Clin. *29*, 773–786.

[S4] Giacino, J. T., Kalmar, K., and Whyte, J. (2004). The JFK Coma Recovery Scale-Revised: measurement characteristics and diagnostic utility. Arch. Phys. Med. Rehabil. *85*, 2020–2029.

[S5] Teasdale, G. M., Pettigrew, L. E., Wilson, J. T., Murray, G., and Jennett, B. (1998). Analyzing outcome of treatment of severe head injury: a review and update on advancing the use of the Glasgow Outcome Scale. J. Neurotrauma *15*, 587–597.

[S6] Avants, B. B., Tustison, N. J., Song, G., Cook, P. A., Klein, A., and Gee, J. C. (2011). A reproducible evaluation of ANTs similarity metric performance in brain image registration. Neuroimage *54*, 2033–2044.

[S7] Phillips, C. L., Bruno, M.-A., Maquet, P., Boly, M., Noirhomme, Q., Schnakers, C., Vanhaudenhuyse, A., Bonjean, M., Hustinx, R., Moonen, G., et al. (2011). "Relevance vector machine" consciousness classifier applied to cerebral metabolism of vegetative and locked-in patients. Neuroimage *56*, 797–808.

[S8] Rorden, C., and Brett, M. (2000). Stereotaxic display of brain lesions. Behav. Neurol. *12*, 191–200.

[S9] Borghammer, P., Jonsdottir, K. Y., Cumming, P., Ostergaard, K., Vang, K., Ashkanian, M., Vafaee, M., Iversen, P., and Gjedde, A. (2008). Normalization in PET group comparison studies--the importance of a valid reference region. Neuroimage *40*, 529–540.

[S10] Lin, J. H. (1991). Divergence Measures Based on the Shannon Entropy. IEEE Trans. Inf. Theory *37*, 145–151.

[S11] Lindholm, H., Brolin, F., Jonsson, C., and Jacobsson, H. (2012). The relation between the blood glucose level and the FDG uptake of tissues at normal PET examinations. EJNMMI Res. *3*, 50–50.

[S12] Backes, H., Walberer, M., Endepols, H., Neumaier, B., Graf, R., Wienhard, K., and Mies, G. (2011). Whiskers area as extracerebral reference tissue for quantification of rat brain metabolism using (18)F-FDG PET: application to focal cerebral ischemia. J. Nucl. Med. *52*, 1252–1260.

[S13] Chen, K., Chen, X., Renaut, R., Alexander, G. E., Bandy, D., Guo, H., and Reiman, E. M. (2007). Characterization of the image-derived carotid artery input function using independent component analysis for the quantitation of [18F] fluorodeoxyglucose positron emission tomography images. Phys. Med. Biol. *52*, 7055–7071.

[S14] Laureys, S., Owen, A. M., and Schiff, N. D. (2004). Brain function in coma, vegetative state, and related disorders. Lancet Neurol. *3*, 537–546.

[S15] Rudolf, J., Ghaemi, M., Ghaemi, M., Haupt, W. F., Szelies, B., and Heiss, W. D. (1999). Cerebral glucose metabolism in acute and persistent vegetative state. J. Neurosurg. Anesthesiol. *11*, 17–24.

[S16] Kuwabara, H., and Gjedde, A. (1991). Measurements of glucose phosphorylation with FDG and PET are not reduced by dephosphorylation of FDG-6-phosphate. J. Nucl. Med. *32*, 692–698.

[S17] Schlünzen, L., Vafaee, M. S., Cold, G. E., Rasmussen, M., Nielsen, J. F., and Gjedde, A. (2004). Effects of subanaesthetic and anaesthetic doses of sevoflurane on regional cerebral blood flow in healthy volunteers. A positron emission tomographic study. Acta Anaesthesiol. Scand. *48*, 1268–1276.

[S18] Linnet K. (1993) Evaluation of Regression Procedures for Methods Comparison Studies. Clin Chem. 39:424–32.